SI Appendix Figures and Tables:

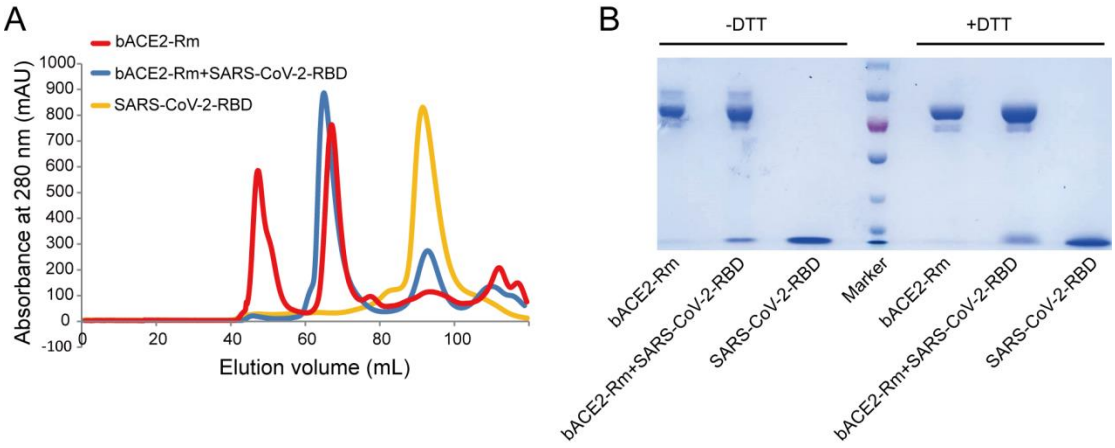

SI Appendix, Fig. S1. Gel filtration profile of SARS-COV-2-RBD/bACE2-Rm complex protein. (A) Gel filtration profiles of bACE2-Rm (red), SARS-COV-2-RBD (yellow) and the bACE2-Rm and SARS-COV-2-RBD complex (blue) were analyzed by size-exclusion chromatography as indicated. (B) The separation profiles of each pooled samples on SDS-PAGE are shown in reducing (+DTT) or non-reducing (-DTT) conditions.

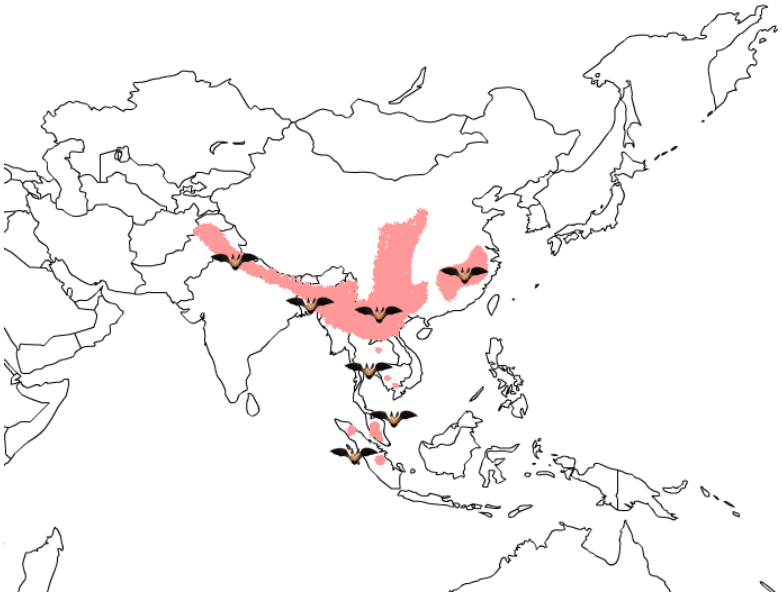

SI Appendix, Fig. S2. The distribution of *Rhinolophus macrotis.* *Rhinolophus macrotis*

mainly distribute in Southeast Asia, such as southern China, Bangladesh, India, Indonesia (Sumatra), Lao People's Democratic Republic, Malaysia (Peninsular Malaysia), Myanmar, Nepal, Pakistan, Thailand, Vietnam, Philippines. This figure is generated based on the findings from Vuong Tan Tu, et al. 2017 J Zool Syst Evol Res. (55) 177-198. doi.org/10.1111/jzs.12169

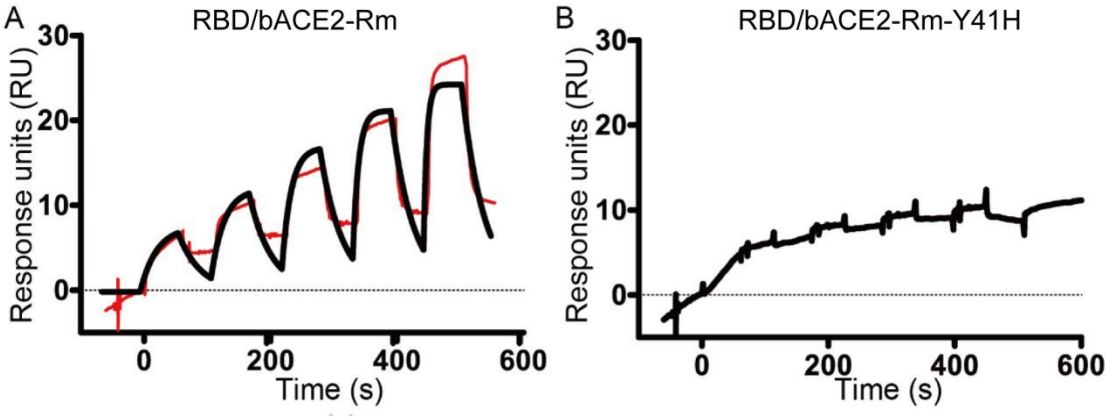

SI Appendix, Fig. S3. SPR analysis of the binding between bACE2-Rm-Y41H mutant and bACE2-Rm-wt. SPR assay characterisation of the binding of wild type bACE2-Rm-wt (A) or bACE2-Rm-Y41H mutant with SARS-COV-2 virus RBD. No substantial binding was observed with bACE2-Rm-Y41H mutant. The fits of the binding curves are shown in red.

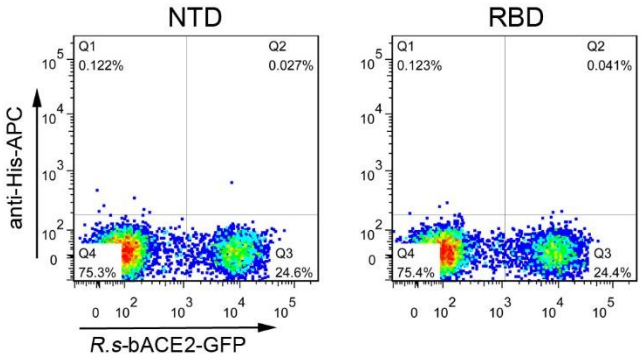

SI Appendix, Fig. S4. Flow cytometry based assay characterizing the binding of the SARS-CoV-2 RBD with the bACE2 from *Rhinolophus sinicus* (R.s-bACE2).

SI Appendix, Table. S1. Binding profiles of SARS-CoV-2-RBD and SARS-CoV-RBD binding to different ACE2s

Interaction pairs	Ka[1](1/Ms)	Kd[2](1/s)	KD(M)
SARS-COV-2-RBD/bACE2-Rm-E.coli	1.02×10^{5}	1.32×10^{-1}	1.30×10^{-6}
SARS-COV-2-RBD/bACE2-Rm-insect	4.61×10^{4}	6.92×10^{-2}	1.50×10^{-6}
SARS-COV-2-RBD/bACE2-Rm-293T cell	4.93×10^{5}	1.37×10^{-1}	2.78×10^{-6}
SARS-CoV-RBD/bACE2-Ra	-	-	-
SARS-COV-2-RBD/hACE2	2.93×10^{5}	5.97×10^{-1}	2.04×10^{-8}

[1] ka, association rate constant.

[2] kd, dissociation rate constant.

SI Appendix, Table. S2. Crystallographic data collection and refinement statistics

	bACE2-Rm/SARS-CoV-2-RBD
Data collection	
Space group	I422
Wavelength (Å)	0.97853
Unit cell dimensions	
a, b, c (Å)	163.20, 163.20, 211.67
α, β, γ ( )	90, 90, 90
Resolution (Å)	50-3.2 (3.31-3.20)*
Unique reflections	24258 (2387)
R_{merge}	0.163/1.790
I/σ	6 (4.3)
Completeness (%)	99.9 (100)
Redundancy	13.4 (13.5)
Refinement	
Resolution (Å)	48.1-3.184
R_{work} / R_{free}	0.2185/0.2708
No. atoms	
Protein	7316
Ligands	1
Water	0
R.m.s. deviations	
Bond lengths (Å)	0.002
Bond angles ( )	0.682
Ramachandran plot	
Favored (%)	99.11
Allowed (%)	0.89

Outliers (%)	0.00

*Values in parentheses are for highest-resolution shell.

SI Appendix, Table. S3. Cryo-EM data collection, refinement and validation statistics of bACE2

	bACE2-Rm
Data collection and processing	
Magnification	130K
Voltage (kV)	300
Electron exposure (e^-/ Å^2)	50
Defocus range (μm)	-1.8 ~ -2.2
Pixel size (Å)	0.99375
Symmetry imposed	C1
Final particle images (no.)	62,289
Map resolution (Å)	3.2
FSC threshold	0.143
Refinement	
Initial model used (PDB code)	6LZG
Model resolution range (Å)	up to 3.2
FSC average (model to map)	
Whole unit cell	0.7702
Around atoms	0.7738
Model composition	
Non-hydrogen atoms	4853
Protein residues	4852
Ligands	1
B factors (Å^2)	
Protein	70.0
Ligand	76.5
R.m.s. deviations	
Bond lengths (Å)	0.002
Bond angles (°)	0.418
Validation	
MolProbity score	1.45
Clashscore	4.88
Poor rotamers (%)	0.00
Ramachandran plot	
Favored (%)	96.80
Allowed (%)	3.20
Outliers (%)	0.00

SI Appendix, Table. S4. Comparison of SARS-CoV-2-RBD binding to hACE2 and bACE2-Rm

SARS-CoV-2-RBD	humanACE2	bACE2-Rm
K417	D30 (4,**1**)	D30 (6,**1**)
G446	Q42 (4, **1**)	E42 (4)
Y449	D38 (9, **1**), Q42 (4, **1**)	D38 (9, **1**), E42 (8, **1**)
Y453	H34 (5, **1**)	S34 (3)
L455	D30 (2), K31 (2), H34 (9)	D30 (7), K31 (3), S34 (2)
F456	T27 (5), D30 (4), K31 (5)	K27 (11), D30 (4), K31 (4)
Y473	T27 (1)	K27 (6, **1**)
A475	S19 (3, **1**), Q24 (4),T27 (2)	E24 (8, **1**), K27 (2)
G476	S19 (4), Q24 (5)	E24 (9)
E484	K31 (1)	K31 (2, **1**)
F486	L79 (2), M82 (9), Y83 (11)	L79 (2), N82 (7), Y83 (8)
N487	Q24 (15, **1**), Y83 (8, **1**)	E24 (16, **1**), Y83 (5, **1**)
Y489	T27 (7), F28 (7), K31 (6), Y83 (1)	K31 (9), F28 (10), Y83 (1, **1**), K27 (4), E24 (1)
F490	K31 (2)	K31(3)
L492		
Q493	K31 (3), H34 (6), E35 (8)	K31 (7), S34 (6), K35 (3)
G496	D38 (5), K353 (7, **1**)	D38 (4), K353 (6, **1**)
Q498	D38 (1), Y41 (8), Q42 (8, **3**), L45 (3)	Y41 (7), D38 (4), E42(3), K353 (2)
P499		K330 (1)
T500	Y41 (7, **1**), L45 (1), N330 (8), D355 (8, **1**), R357 (3)	K330 (11, **1**), Y41 (10, **1**), L45 (3), D355 (9), R357 (3)
N501	Y41 (8, **1**), K353 (11)	Y41 (14, **1**), K330 (1), K353 (11)
G502	K353 (4, **1**), G354 (7), D355 (1)	K353 (6, **1**), G354 (6), D355 (1)
Y505	E37 (7), K353 (28), G354 (4), R393 (1)	K353 (27), E37 (8, **1**) , R393 (2), G354 (2)
Total	288, 16	311,14

The numbers in parentheses of hACE2 and bACE2-Rm residues represent the number of vdw contacts between the indicated residues with SARS-CoV-2-RBD. The numbers with underline suggest numbers of potential H-bonds between the pairs of residues. wdw contact was analyzed at a cutoff of 4.5 Å and H-bonds at a cutoff of 3.5 Å.

SI Appendix, Table. S5.Conservation analysis of the residues involved in ACE2 binding to SARS-CoV-2-RBD among 31 bats

	24	27	28	30	31	34	35	37	38	41	42	45	79	82	83	330	353	354	355	357	393	Substitutions
ADN93471|Rhinolophus_macrotis	E	K	F	D	K	S	K	E	D	Y	E	L	L	N	Y	K	K	G	D	R	R	
QMQ39222.1|Rhinolophus affinis	R	I	F	D	N	R	E	E	E	Y	Q	L	L	N	Y	N	K	G	D	R	R	7
XP_023609439|Myotis_lucifugus	K	I	F	E	N	S	K	E	D	H	E	L	L	T	Y	N	K	G	D	R	R	7
ADJ19219|Rousettus_leschenaultii	L	T	F	E	K	T	E	E	D	Y	Q	L	L	T	Y	K	K	G	D	R	R	7
BAH02663|Rhinolophus_ferrumequinum	L	K	F	D	D	S	E	E	N	H	Q	L	L	N	F	N	K	G	D	R	R	8
ADN93472|Rhinolophus_sinicus	E	I	F	D	K	T	K	E	D	H	Q	L	L	N	Y	N	K	G	D	R	R	5
ADN93477|Rhinolophus_pusillus	K	K	F	N	D	S	E	E	D	Y	Q	L	L	N	Y	N	K	G	D	R	R	6
ACM45790|Rhinolophus_ferrumequinum	L	T	F	E	K	T	E	E	D	Y	Q	L	L	T	Y	K	K	G	D	R	R	7
BAF50705|Rousettus_leschenaultii	L	T	F	E	K	T	E	E	D	Y	Q	L	L	T	Y	K	K	G	D	R	R	7
XP_015974412|Rousettus_aegyptiacus	L	T	F	E	K	T	E	E	D	Y	Q	L	L	T	Y	K	K	G	D	R	R	7
XP_011361275|Pteropus_vampyrus	L	T	F	E	K	T	E	E	D	Y	Q	L	L	A	Y	K	K	G	D	R	K	7
XP_006911709|Pteropus_alecto	L	T	F	E	K	T	E	E	D	Y	Q	L	L	A	Y	K	K	G	D	R	K	7
XP_019522936|Hipposideros_armiger	L	E	F	D	K	T	E	E	D	H	L	L	R	D	Y	N	K	G	D	R	R	8
ADN93470|Rhinolophus_ferrumequinum	L	K	F	D	D	S	E	E	N	H	Q	L	L	N	F	N	K	G	D	R	R	8
ALJ94034|Rhinolophus_landeri	L	T	F	D	D	S	A	E	N	Y	Q	L	H	N	F	N	K	G	D	R	R	9
ALJ94035|Rhinolophus_alcyone	L	I	F	D	N	S	E	E	N	H	Q	L	H	N	F	N	K	G	D	R	R	10
ABU54053|Rhinolophus_pearsonii	R	T	F	D	K	H	E	E	D	H	Q	L	L	D	Y	N	K	D	D	R	R	9
ACT66275|Rhinolophus_sinicus	L	I	F	D	E	S	E	E	N	Y	Q	L	L	N	Y	N	K	G	D	R	R	7
ADN93475|Rhinolophus_sinicus	R	T	F	D	E	S	E	E	N	Y	Q	L	L	N	Y	N	K	G	D	R	R	7
AGZ48803|Rhinolophus_sinicus	E	M	F	D	K	T	K	E	D	H	Q	L	L	N	Y	N	K	K	D	R	R	6
XP_028378317|Phyllostomus_discolor	D	K	F	E	N	N	E	E	E	Y	Q	L	L	N	Y	N	K	K	D	R	R	9
XP_024425698|Desmodus_rotundus	E	T	F	E	N	T	E	E	E	Y	Q	L	I	T	Y	N	N	G	D	R	R	11
XP_016058453|Miniopterus_natalensis	K	K	F	E	G	S	Q	E	D	F	E	L	L	I	Y	N	K	N	D	R	R	8
ACT66266|Pipistrellus_abramus	E	R	F	V	K	H	E	E	N	H	E	L	I	G	Y	D	K	N	D	R	R	10

XP_027986092|Eptesicus_fuscus	N	I	F	E	N	S	E	E	D	H	E	L	L	T	F	N	K	N	D	R	R	10
XP_008153150|Eptesicus_fuscus	N	I	F	E	N	S	E	E	D	H	E	L	L	T	Y	N	K	G	D	R	R	7
XP_015426919|Myotis_davidii	K	I	F	D	N	S	K	E	D	H	E	L	L	T	Y	N	K	G	D	R	R	6
XP_006775273|Myotis_davidii	K	I	F	D	N	S	K	E	D	H	E	L	L	T	Y	N	K	G	D	R	R	6
XP_023609437|Myotis_lucifugus	K	I	F	E	N	S	K	E	D	H	E	L	L	T	Y	N	K	G	D	R	R	7
XP_014399783|Myotis_brandtii	K	I	F	E	N	S	K	E	D	H	E	L	L	T	Y	N	K	G	D	R	R	7
XP_014399782|Myotis_brandtii	K	I	F	E	N	S	K	E	D	H	E	L	L	T	Y	N	K	G	D	R	R	7
XP_014399780|Myotis_brandtii	K	I	F	E	N	S	K	E	D	H	E	L	L	T	Y	N	K	G	D	R	R	7

Red letters indicate the substitutions in the ACE2 of 31 bats.